

## Rapid oscillations in the organic conductor $(\text{TMTSF})_2\text{ClO}_4$

S. Uji, T. Terashima, and H. Aoki

*Tsukuba Magnet Laboratories, National Research Institute for Metals, Tsukuba, Ibaraki 305, Japan*

J. S. Brooks

*Department of Physics, Florida State University, Tallahassee, Florida 32306-4005*

M. Tokumoto

*Electrotechnical Laboratory, Tsukuba, Ibaraki 305, Japan*

S. Takasaki, J. Yamada, and H. Anzai

*Himeji Institute of Technology, Akahogun, Hyogo 678-12, Japan*

(Received 28 November 1995)

The magnetoresistance measurements for the quasi-one-dimensional conductor  $(\text{TMTSF})_2\text{ClO}_4$  have been performed over a wide temperature range in order to investigate the mechanism of the anomalous rapid oscillation (RO) behavior. The dependences of the RO's on the electric current and magnetic-field directions, cooling rate, and temperature are investigated in the low-field metallic (M) and the spin-density-wave (SDW) phases for the same crystal. We conclude that the mechanisms of the RO's are different in the two phases. The RO in the M phase is caused by the Stark quantum interference effect—however the mechanism of the RO in the SDW phase is still an open question. [S0163-1829(96)01322-7]

### I. INTRODUCTION

The quasi-one-dimensional organic conductors  $(\text{TMTSF})_2X$ , where TMTSF denotes tetramethyltetraselenafulvalene and  $X=\text{ClO}_4$ ,  $\text{PF}_6$ ,  $\text{RO}_4$ , etc., have many interesting properties such as anion ordering (AO), superconductivity, quantum Hall effect, rapid oscillation (RO), and field-induced spin-density-wave (FISDW) transitions.<sup>1</sup> The stacked platelike TMTSF molecules yield a highly anisotropic Fermi surface with only open sheets. For the slowly cooled  $\text{ClO}_4$  salt, the AO takes place at 24 K, which causes a superlattice potential with a wave vector  $\mathbf{Q}=(0,\pi/b,0)$ . The potential separates the original Fermi surface into two zones, which is illustrated in Fig. 1(a).

The magnetic field along the  $c^*$  axis leads to the FISDW formation, which is characterized by plateaus in the Hall resistance. This cascadelike transition is understood in terms of the field-dependent nesting vector which readjusts itself to maintain the Fermi energy in the energy gap. For the  $\text{ClO}_4$  salt, the final FISDW transition occurs at about 8 T ( $H_c$ ). Recently, a phase diagram was proposed, where a different SDW phase is present above 28 T as shown in Fig. 1(c).<sup>2</sup> The superconducting phase, which is denoted by  $S$ , exists in a low-field region below about 1 K. The RO, which is considered to be a new type of quantum oscillation, is observable not only in the M phase but also in the SDW phase. The RO is a periodic function of the inverse field, which is very similar to the Shubnikov-de Haas (SdH) or de Haas-van Alphen (dHvA) effects.<sup>3-9</sup> There is a substantial body of literature concerned with the mechanism of the RO, but no theory has been entirely consistent with the experimental results.

In order to further investigate the mechanism of the RO, we have made extensive measurements of the magnetoresis-

tance over a wide temperature range above and below  $H_c$  for a slowly cooled  $\text{ClO}_4$  sample.

### II. EXPERIMENT

The resistance was measured with electric current along the highly conducting  $a$  axis and the least conducting  $c^*$  axis for the same sample. The experiments were done by using a dilution refrigerator and a  $^4\text{He}$  cryostat with a superconducting magnet. Six gold wires ( $\phi 10\ \mu\text{m}$ ) were attached to the sample using silver paint. The sample was slowly cooled in the temperature range from 32 to 18 K to obtain a well ordered state of the  $\text{ClO}_4$  anions. The cooling rate dependences of the resistance and the RO were also investigated. A sharp superconducting transition was found at about 1 K. In this paper, we present the data from one sample.

### III. RESULTS

#### A. Cooling rate and current direction dependences

Figure 2 shows the resistance as a function of magnetic field ( $H\parallel c^*$ ) for three different cooling rates from 9 to 50 mK/min, which are the averaged values in the range from 32 to 18 K. The transition to the last SDW phase takes place at about 8 T, where the resistance suddenly increases. The transition field  $H_c$  is not very sensitive to the cooling rate. The nonoscillatory background of the resistance increases as the cooling rate decreases. The RO is evident above 11 T. The Fourier transform (FT) spectra of the RO's between 10 and 13.5 T are shown in the inset. We note that the second harmonic with the frequency of  $2F$  ( $=530$  T) is evident in addition to the fundamental oscillation with  $F$  ( $=265$  T). Both the amplitudes increase with decreasing cooling rate. The

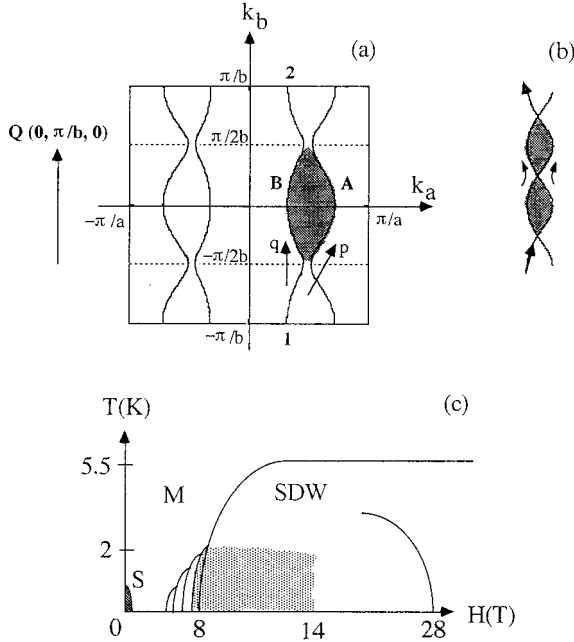


FIG. 1. (a) Schematic picture of the Fermi surface in  $(\text{TMTSF})_2\text{ClO}_4$  in the presence of the anion order. The hatched area corresponds to the frequency of the magnetoresistance oscillation due to the Stark effect. (b) Area enclosed by two longer trajectories is shown. This interference produces the second harmonic. (c) Schematic  $T$ - $H$  phase diagram (Ref. 2). The hatched area shows the field region where the hysteresis of the magnetoresistance is evident.

amplitude of the second harmonic is found to be less sensitive to the cooling rate. This behavior agrees with the pulse-field data by Agosta *et al.*<sup>10</sup> For 50 mK/min, only the second harmonic is evident. The large difference between the 9 and 10 mK/min data is probably due to two facts; One is that the sample was cooled much more smoothly for the 9 mK/min cooling process than for the 10 mK/min process. The other one is that the temperature was raised only to 35 K to begin the 9 mK/min cooling after the 10 mK/min experiment.

Figure 3 shows the resistance for magnetic fields ( $H \parallel c^*$ ) up to 14 T for  $I \parallel a$  and  $I \parallel c^*$  at 3.2 K. The transition to the last SDW phase is seen at about 9.5 T. The  $dR/dH$  curves are shown in the inset. The RO is observable for both  $I \parallel a$  and  $I \parallel c^*$  in the SDW phase, but seen only for  $I \parallel a$  in the M phase. Only in the SDW phase, the second harmonic is evident in addition to the fundamental oscillation.<sup>6,10</sup> The relative amplitude of the second harmonic to the fundamental oscillation is larger for  $I \parallel a$  than for  $I \parallel c^*$ .

### B. Temperature dependence

Figure 4 shows the field dependence of the  $a$ -axis resistance at various temperatures for the down sweep ( $H \parallel c^*$ ). The magnetoresistance shows hysteresis in a broad field range as presented later. The transition field to the final SDW phase increases with increasing temperature, which is in agreement with the previous reports. The resistance has a broad maximum at about 11 T below 1 K. Below 1 K, the RO is not evident, but above 1 K, we can see the RO clearly.

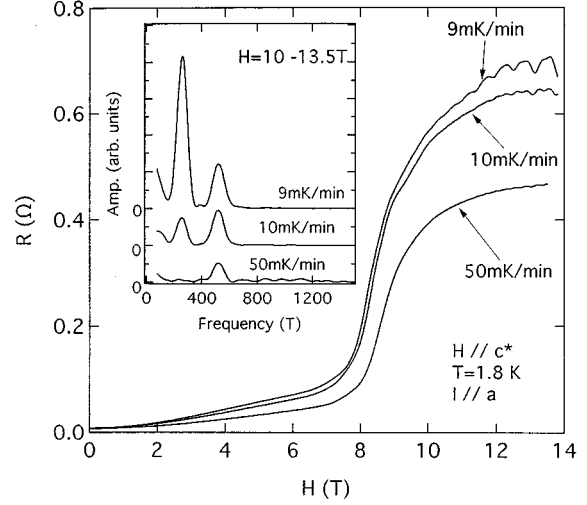


FIG. 2. Resistance for three different cooling rates for  $I \parallel c^*$  and  $I \parallel a$ . The magnetic field is parallel to the  $c^*$  axis. The inset shows the FT spectra of the oscillations in the field region between 10 and 13.5 T.

Above 5 K, the SDW transition does not appear in this field range, whereas the RO is still observed.

To see the RO more clearly, we plotted the  $dR/d(1/H)$  curves normalized by the nonoscillatory background  $R_0$  at various temperatures for  $I \parallel a$  and  $H \parallel c^*$  in Fig. 5. The last SDW transition fields are shown by arrows. The oscillation amplitude in the SDW phase increases as a function of field more rapidly than in the M phase, which agrees with previous work.<sup>6</sup> The field dependence of the amplitude in the SDW phase is the largest at 2.1 K.

Figure 6 shows the FT spectra of the  $dR/d(1/H)$  curves for the field range from 10.6 to 13.7 T. At 3.5 and 4.2 K, the SDW transition appears in this field region. In the SDW phase ( $T < 3.5$  K), we see the strong second harmonic in addition to the fundamental oscillation.

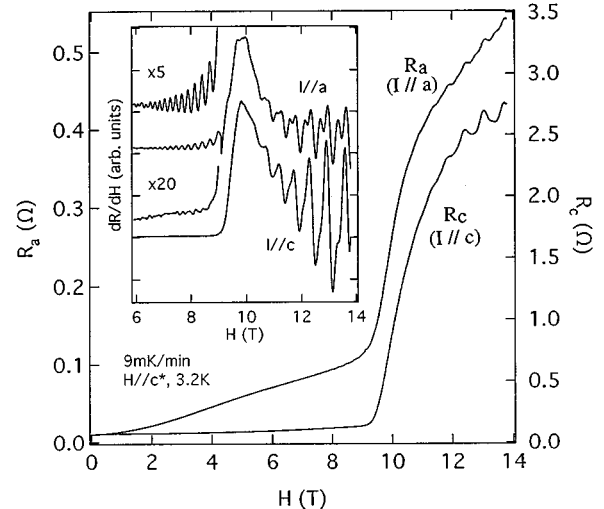


FIG. 3. Resistance for  $I \parallel a$  and  $I \parallel c^*$  at 3.2 K. The field is parallel to the  $c^*$  axis. The  $dR/dH$  curves are shown in the inset.

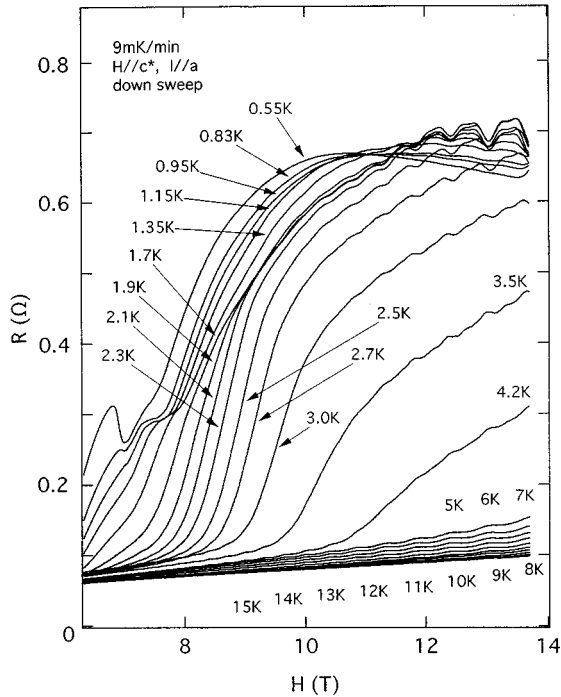


FIG. 4. Magnetic-field dependence of the resistance for  $H||a$  and  $H||c^*$  at various temperatures. The data was taken for the down sweep.

Figure 7 presents the temperature dependence of the oscillation amplitude normalized by the nonoscillatory background  $R_0$ . The closed and open circles denote the amplitudes of the fundamental oscillation and second harmonic in the SDW phase ( $H=10.6-13.7$  T), respectively. We note that both amplitudes have maxima at the same temperature (2.1 K), where the RO amplitude has the largest field depen-

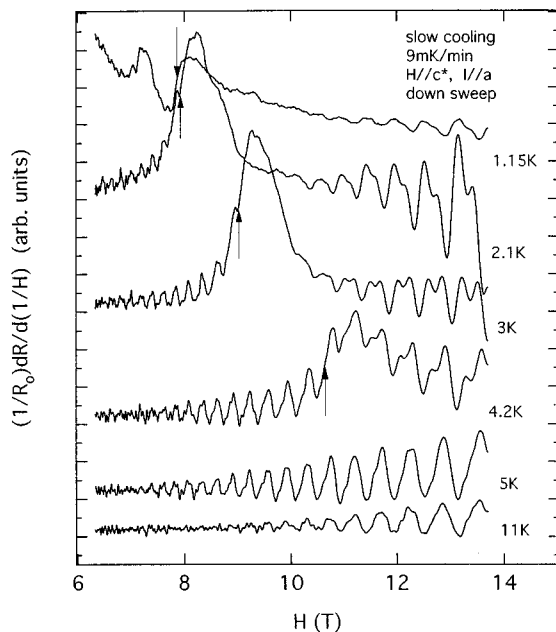


FIG. 5.  $dR/d(1/H)$  curves at various temperatures for  $H||a$  and  $H||c^*$ . The arrows show the transition field to the last SDW phase.

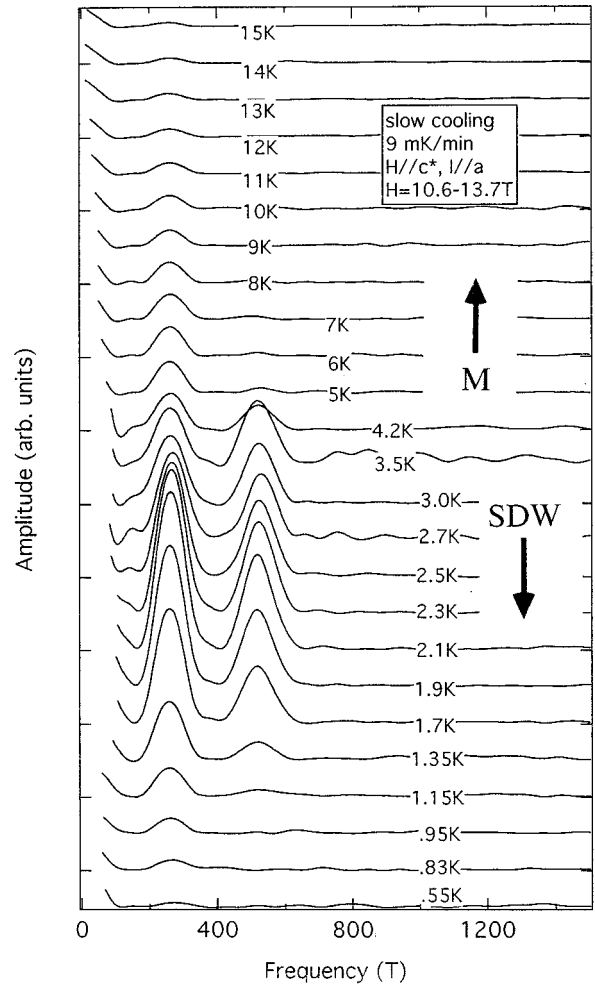


FIG. 6. FT spectra of the  $dR/d(1/H)$  curves for the field range from 10.6 to 13.7 T. At 3.5 and 4.2 K, the spectra are of the transient region from the M phase to the SDW phase.

dependence. The amplitudes steeply decrease below 2.1 K. Similar behavior has been reported by a few groups,<sup>5,10</sup> but the temperatures where the amplitudes have maxima range from 2.5 to 3 K with broader peaks. The difference suggests that the temperature dependence is sensitive to the cooling rate and/or the sample quality. The closed and open triangles (Fig. 7) show the FT amplitudes of the fundamental oscillation and second harmonic in the M phase ( $H=10.6-13.7$  T), respectively. The squares and crosses show the FT amplitudes in the M phase in the field ranges  $H=6-9$  T and  $H=5-7$  T, respectively. The amplitudes in both field regions are normalized at 6 and 3.3 K, respectively, so that the overall feature is easily viewed. The amplitude in the M phase increases monotonically with decreasing temperature and has no anomalous peak in contrast to that in the SDW phase. In the higher field region ( $H>25$  T), the amplitude is reported to have a similar monotonic temperature dependence.<sup>5</sup> In a recent pulsed magnetic-field study, a similar temperature dependence and small harmonic ratio are found above 25 T.<sup>11</sup>

Figure 8 presents the resistance for the up- and down-field sweeps at various temperatures. This is the data for the 10 mK/min sample. The similar behavior is also observed for

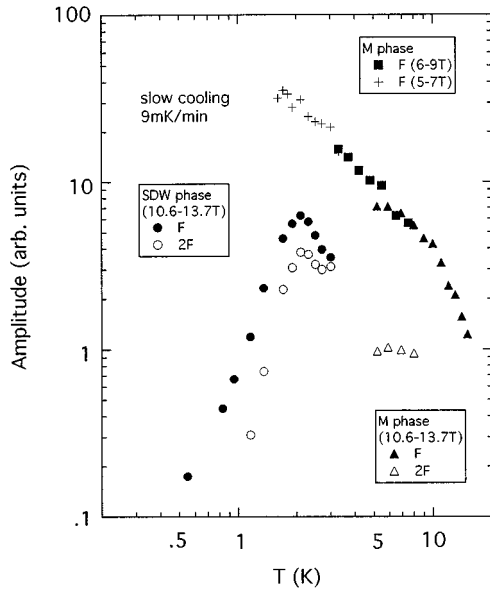


FIG. 7. Temperature dependences of the RO amplitudes. See text for details.

the 9 mK/min experiment. We note that the hysteresis is seen in a wide field region from 6 to 14 T below 2.1 K. This observation is consistent with previous results.<sup>11-13</sup> A full detail of the hysteretic behavior in many thermodynamical quantities was recently reported by Scheven *et al.*<sup>14</sup> The hysteretic behavior in Fig. 8 seems anomalous, because the down-sweep data is not simply given by the upward shift of

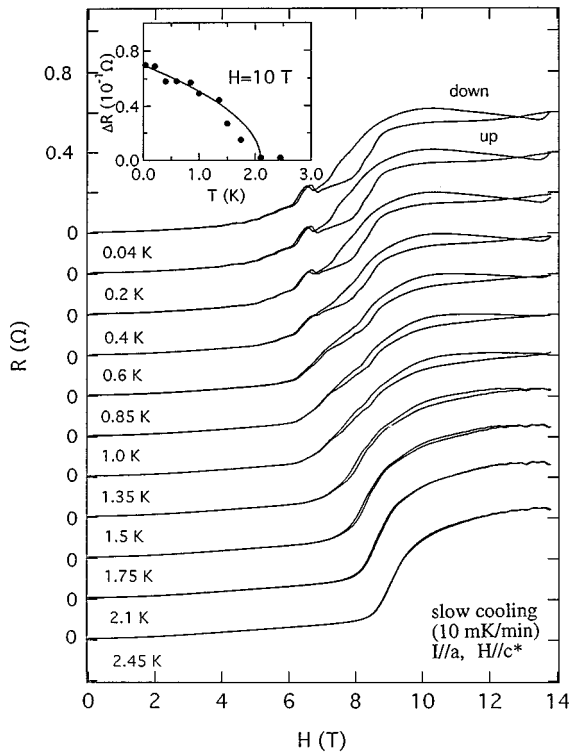


FIG. 8. Resistance for  $I \parallel a$  at various temperatures. The inset shows the hysteretic part of the resistance at 10 T.

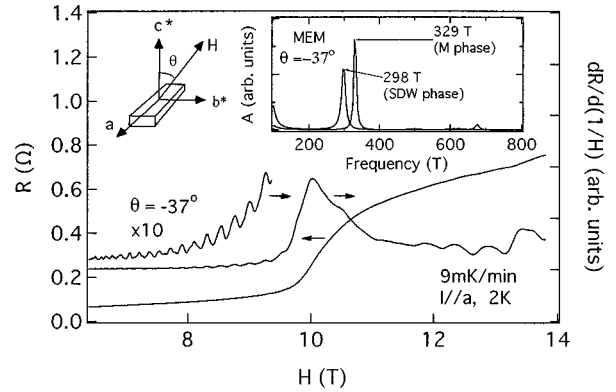


FIG. 9. Resistance and the derivative curve for  $\theta = -37^\circ$  at 2 K. The inset shows the power spectra in the M and SDW phases calculated by MEM.

the up-sweep data. The hysteresis becomes small as the field is tilted from the  $c^*$  axis to the  $b^*$  axis. The inset shows the hysteretic part of the resistance  $\Delta R$  at 10 T.  $\Delta R$  is very small above 2.1 K and increases with decreasing temperature below 2.1 K. This behavior closely correlates with the steep decrease of the RO amplitude in the SDW phase (Fig. 7), which will be discussed later.

### C. Angular dependence

The angular dependence of the RO was carefully measured up to 14 T at 2 K. At 2 K, only the final FISDW transition is evident. Figure 9 shows the resistance for  $\theta = -37^\circ$ , where  $\theta$  is the angle between the  $c^*$  axis and the magnetic field. The power spectra of the RO's in both M and SDW phases are calculated by the maximum entropy method<sup>14</sup> (MEM) to improve the resolution (inset of Fig. 9). The frequency in the SDW phase is apparently lower than that in the M phase.

The angular dependence of the frequencies in both phases and the transition field  $H_c$  is shown in Fig. 10. The frequencies in the SDW phase for  $|\theta| > 30^\circ$  are scattered because of the limited field region for the MEM calculation. The frequencies in the M phase and  $H_c$  exactly follow the  $1/\cos(\theta)$

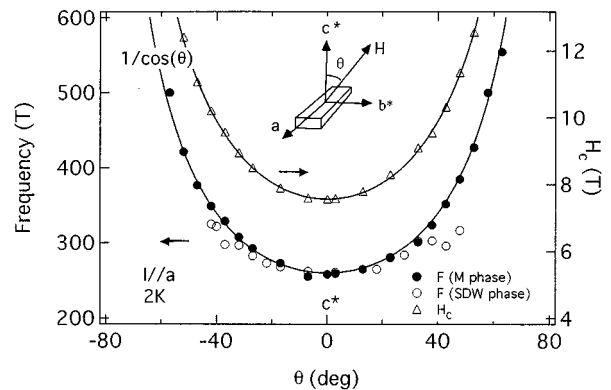


FIG. 10. Angular dependences of the frequencies of the RO in the M phase (closed circles) and the SDW phase (open circles), and the transition field  $H_c$  at 2 K.

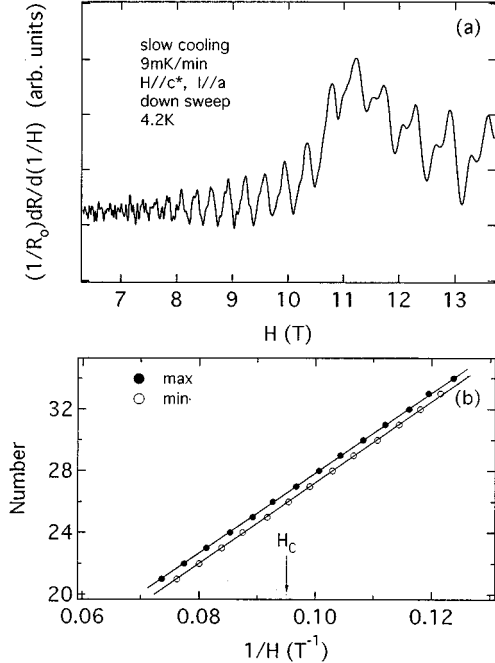


FIG. 11. (a)  $dR/d(1/H)$  curve normalized by the nonoscillatory background  $R_0$  at 4.2 K. The SDW transition takes place at 10.5 T. (b) The indices of the minimum and maximum of the RO are plotted as a function of the inverse field.

dependence in the whole angle region. For  $|\theta| < 35^\circ$ , the frequencies in the SDW phase coincide with those in the M phase within experimental limits. However, we note that the frequencies in the SDW phase show a systematic deviation from the  $1/\cos(\theta)$  dependence for  $|\theta| > 35^\circ$ .

The angular dependence of the frequency is expected to be sensitive to the shape of the Fermi surface. Therefore, the difference of the angular dependences may suggest that the Fermi surfaces in both phases have different dispersions along the  $c^*$  axis. The angular dependence of the frequency in the SDW phase has been measured by a few groups<sup>3,4</sup> and was reported to follow the  $1/\cos(\theta)$  dependence up to about  $50^\circ$ . The reason for the disagreement is unclear.

#### D. Phase of RO

To investigate the phase difference of the RO between the M and SDW phases, the RO was carefully measured for  $H//c^*$ . The  $dR/d(1/H)$  curve normalized by the nonoscillatory background  $R_0$  is shown in Fig. 11(a). The SDW transition is seen at 10.5 T. The indices of the minimum and maximum of the RO are plotted as a function of the inverse field in Fig. 11(b). Each data lies on a straight line in the whole field region. This behavior shows that the phase and frequency are exactly the same in both phases for  $H//c^*$ . The result is in agreement with the previous report by Yan *et al.*<sup>6</sup>

### IV. DISCUSSION

#### A. Stark quantum interference effect

As we have shown, the RO's in the SDW and M phases have different properties in many aspects (wave shape, and

current direction, temperature, field, and angular dependences). The differences show that the RO's have different origins between the M and SDW phases.

Yan *et al.*<sup>6</sup> attributed the RO observed in a wide field region (M and SDW phases) to the Stark quantum interference effect.<sup>15</sup> The possibility of the Stark effect in the SDW phase was excluded because of the observation in the thermodynamic quantities.<sup>7-9</sup> However, it is likely that the RO in the M phase is caused by the Stark effect, because it has been found only in the resistance in contrast to that in the SDW phase.

The Stark effect takes place when an electron proceeds along two alternative trajectories labeled by A and B from the point 1 to 2 as shown in Fig. 1(a). The transmission probability of the electron from the point 1 to 2 is given by

$$|\langle 1|2\rangle|^2 = p^2 + (1-p)^2 - 2p(1-p)\cos(\phi_1 - \phi_2),$$

$$\phi_1 - \phi_2 = \frac{\hbar c A}{eH},$$

where  $A$  is the  $k$ -space area of the loop [hatched area in Fig. 1(a)]. The second term is the interference term. The quantity  $p$  is the probability that the magnetic breakdown occurs at the zone boundary ( $|k_b| = \pi/2b$ ), and  $1-p$  is the probability of the Bragg reflection. The probability  $p$  is expressed as

$$p = \exp(-\Delta/H),$$

$$\Delta \cong \frac{m^* c E_g^2}{\hbar e E_F},$$

where  $E_g$  and  $E_F$  are the energy gap between the two energy bands and the Fermi energy, respectively. Here the phase coherence is a prerequisite for the presence of the interference. However, the phase coherence of the electronic state is broken by scattering characterized by the time  $\tau$ . Therefore, the oscillation amplitude is reduced by the factor  $K_L = \exp(-t_L/\tau)$  on each path segment  $L$ , which is traveled by the electron in time  $t_L$ . This factor has the same form as the Dingle reduction factor in the SdH or dHvA effects<sup>16</sup> because  $t_L \propto 1/H$  and  $\tau \propto 1/x$ , where  $x$  is the Dingle temperature. This factor is rewritten as  $\exp(-\pi/\omega_c \tau)$ , where  $\omega_c = eHv_F b/\hbar c$ .  $v_F$  is the Fermi velocity and  $b$  is the lattice constant of the  $b$  axis. The oscillation amplitude  $I_{\text{osc}}$  is consequently expected to have a form

$$I_{\text{osc}} \approx 2p(1-p)\exp\left(-\frac{\pi}{\omega_c \tau}\right).$$

At a fixed temperature, the field dependence of the RO amplitude is calculated by the above expression on the assumption of the field-independent scattering time. Figure 12(a) shows the RO of the M phase observed at 5.2 K. The amplitude normalized by the nonoscillatory background  $R_0$  is presented in Fig. 12(b). The solid line in Fig. 12(b) shows the fitted result with the reasonable values of the parameters ( $\tau \cong 1.5 \times 10^{-12}$  sec and  $E_g \cong 4.5$  meV). Here we assumed the free-electron mass ( $m^* = m_0$ ) and  $E_F = 0.1$  eV. The agreement with the experimental result seems satisfactory.

The resistance increases with increasing temperature. The temperature dependence of the scattering time  $\tau$  can be de-

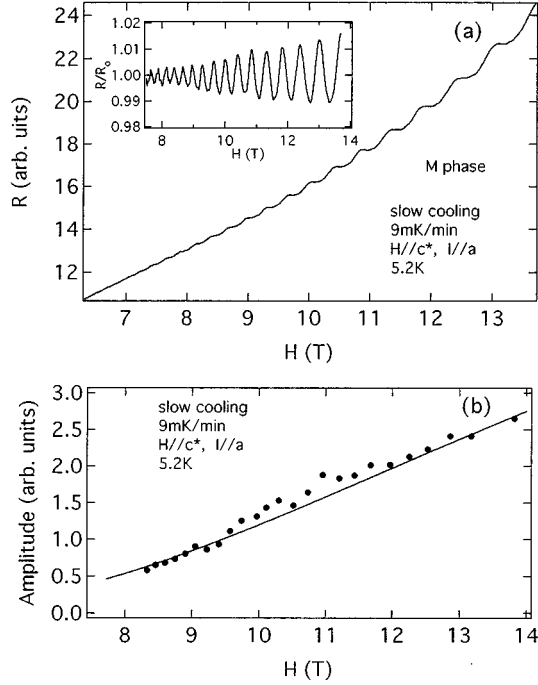


FIG. 12. (a) RO in the M phase observed at 5.2 K. The inset shows the oscillatory component normalized by the nonoscillatory background. (b) Field dependence of the RO amplitude at 5.2 K. The solid line shows the fitted result with the parameters  $\tau \cong 1.5 \times 10^{-12}$  sec and  $E_g \cong 4.5$  meV on the assumption of the free electron mass ( $m^* = m_0$ ) and  $E_F = 0.1$  eV.

duced from the resistivity ( $\rho = m/ne^2\tau$ ). The scattering time  $\tau$  in the Stark effect is not necessarily equal to that deduced from the resistance, but we can expect that both have the similar temperature dependence. Assuming that the temperature dependence of  $\tau$  in the Stark effect is equal to that obtained from the resistance, we can calculate the temperature dependence of the RO amplitude. Figure 13 shows the temperature dependence of the RO amplitude (triangles) in the M phase ( $H = 10.6\text{--}13.7$  T) and the calculated result (a solid line). The experimental result is found to be explained well by the above model. The temperature dependence of the scattering time  $\tau$  deduced from the resistance curve (inset) is also shown. The scattering time is longer by a factor of 2–3 than that obtained from the fitting in Fig. 12(b). The difference may be due to the simplified assumption.

For the Stark effect, the second harmonic arises from the interference between the longer trajectories as shown in Fig. 1(b). The amplitude of the second harmonic should be suppressed much more than the fundamental oscillation because of the additional reduction factors due to the Bragg reflection and more electron scattering due to the longer trajectories. Therefore, the very small amplitude of the second harmonic in the M phase is also consistent with the Stark effect. It is known that the Stark effect is dominant in  $R_b$  rather than in  $R_a$  when there are open orbits along the  $a$  axis as shown in Fig. 1(a). However, the  $R_b$  component is observed even for the  $R_a$  measurements because the electric contact configuration is not ideal and the  $a$  axis is not exactly perpendicular to the open orbits. For  $H \parallel c^*$ , the Stark effect is expected to be very small, which is consistent with the result shown in Fig. 3.

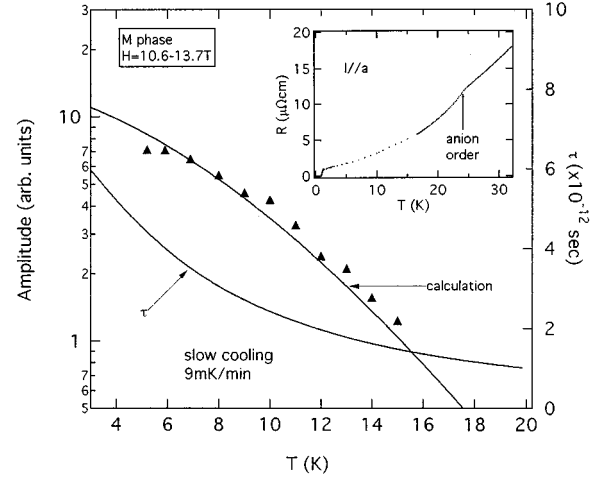


FIG. 13. The temperature dependence of the RO amplitude determined from the FT peak in the field range between 10.6 and 13.7 T. The solid line is the calculated result with the scattering time  $\tau$  deduced from the resistance. The inset shows the temperature dependence of the  $a$ -axis resistance.

For  $(\text{TMTSF})_2\text{PF}_6$  salt, the RO is observed only in the FISDW phase but not in the M phase. For the  $\text{PF}_6$  salt, the superlattice along the  $b$  axis is absent because of the octahedral symmetry of the anion in contrast to the  $\text{ClO}_4$  anion. Therefore, the Stark effect is not expected for the  $\text{PF}_6$  salt.

Recently, a mechanism of the RO in the M phase was proposed by Lebed.<sup>17</sup> The oscillation of resistance was calculated on the basis of the field-dependent electron-electron scattering in the presence of the anion order. According to the theory, the oscillation amplitude has  $1/T^2$  and  $1/T^4$  terms for  $T > T^*$ , where  $T^*$  is a characteristic temperature depending on  $H$ . However, this dependence seems inconsistent with our experimental result (Fig. 7).

## B. Temperature dependence of the RO in the SDW phase

As shown in Fig. 1(c), there is only one FISDW transition ( $H_c > 8$  T) above 2 K, but a cascade of transitions below  $\sim 2$  K. The cascade is associated with hysteresis, and is the first order in nature. As shown in Fig. 8, the hysteresis in the resistance is observed in a wide field region [Fig. 1(c)] below  $\sim 2$  K. The hysteresis suggests the coexistence of different subphases, i.e., the last and the neighboring SDW phases. It is expected that the nucleation of the domain of the last SDW phase starts at  $\sim 8$  T and that the domain increases as the field increases. Such domain structure should cause an additional scattering of the conduction electrons at the boundaries of the domains. The increase of the hysteresis below 2 K (Fig. 8) may suggest that the phase is more inhomogeneous at lower temperatures, e.g., there are more domains, or that the domains increase more slowly as a function of field. In this case, the RO amplitude should be suppressed by this additional scattering at lower temperatures. This picture seems consistent with the steep decrease of the RO amplitude in the SDW phase below 2.1 K (Fig. 7). On the other

hand, above 2 K, neither hysteresis nor the cascade transition are evident, so the SDW phase is expected to be homogeneous in this region. Therefore, the additional scattering above 2 K should not be present. Above 2 K, the RO amplitude decreases with increasing temperature. This may be the intrinsic temperature dependence of the RO amplitude. The field dependence of the RO amplitude in the SDW phase seems largest at 2.1 K (Fig. 5). At present, it is not clear how this field dependence fits into the above picture.

The Stark effect is still possible in the SDW phase. However, the amplitude of the oscillation in the SDW phase should be suppressed, because there exist the energy gaps due to the nesting of the FS. Moreover, the RO has been observed in many thermodynamical quantities in the SDW phase. Therefore, the Stark effect is not the main mechanism of the RO in the SDW phase.

## V. SUMMARY

We have found many differences in the behavior of the RO's between the M and SDW phases. The analysis further shows that the mechanisms of the RO's in the two phases are different. In the M phase, all the behavior of the RO is consistently understood in terms of the Stark quantum interference effect. In the SDW phase, the RO has complicated characteristics and the mechanism of the RO is still an open question.

## ACKNOWLEDGMENTS

We would like to thank P. M. Chaikin, T. Osada, A. G. Lebed, and S. McKernan for helpful discussions. The experiments were carried out at Tsukuba Magnet Laboratories in National Research Institute for Metals. This study is partially supported by NSF DMR 92-14889.

- 
- <sup>1</sup>For a review, see T. Ishiguro and K. Yamaji, *Organic Superconductors* (Springer-Verlag, Berlin, 1990).
- <sup>2</sup>S. K. McKernan, S. T. Hannahs, U. M. Scheven, G. M. Danner, and P. M. Chaikin, *Phys. Rev. Lett.* **75**, 1630 (1995).
- <sup>3</sup>H. Bando, K. Oshima, M. Suzuki, H. Kobayashi, and G. Saito, *J. Phys. Soc. Jpn.* **51**, 2711 (1982).
- <sup>4</sup>J. P. Ulmet, L. Bachere, and S. Askenazy, *Solid State Commun.* **58**, 753 (1986).
- <sup>5</sup>T. Osada, N. Miura, and G. Saito, *Solid State Commun.* **60**, 441 (1986).
- <sup>6</sup>X. Yan, M. J. Naughton, R. V. Chamberlin, S. Y. Hsu, L. Y. Chiang, J. S. Brooks, and P. M. Chaikin, *Phys. Rev. B* **36**, 1799 (1987).
- <sup>7</sup>N. A. Fortune, J. S. Brooks, M. J. Graf, G. Montambaux, L. Y. Chiang, J. A. A. Perenboom, and D. Althof, *Phys. Rev. Lett.* **64**, 2054 (1990).
- <sup>8</sup>R. C. Yu, L. Chiang, R. Upasani, and P. M. Chaikin, *Phys. Rev. Lett.* **65**, 2458 (1990).
- <sup>9</sup>X. D. Shi, W. Kang, and P. M. Chaikin, *Phys. Rev. B* **50**, 1984 (1994).
- <sup>10</sup>C. C. Agosta, D. A. Howe, M. A. Antia, S. A. Ivanov, C. H. Mielke, and F. M. Morgan, in *High Magnetic Fields in the Physics of Semiconductors*, edited by D. Heiman (World Scientific, Singapore, 1995), p. 738.
- <sup>11</sup>J. S. Brooks, R. G. Clark, R. H. McKenzie, R. Newbury, R. P. Starrett, A. V. Skougarevsky, M. Tokumoto, S. Takasaki, J. Yamada, H. Anzai, and S. Uji, following paper, *Phys. Rev. B* **53**, 14 406 (1996).
- <sup>12</sup>K. Oshima, M. Suzuki, K. Kikuchi, H. Kuroda, I. Ikemoto, and K. Kobayashi, *J. Phys. Soc. Jpn.* **10**, 3295 (1984).
- <sup>13</sup>T. I. Sigfusson, K. P. Emilsson, and P. Mattocks, *Phys. Rev. B* **46**, 10 446 (1992).
- <sup>14</sup>U. M. Scheven, E. I. Chashechkina, E. Lee, and P. M. Chaikin, *Phys. Rev. B* **52**, 3484 (1995).
- <sup>15</sup>R. W. Stark and C. B. Friedberg, *J. Low Temp. Phys.* **14**, 111 (1974).
- <sup>16</sup>D. Shoenberg, *Magnetic Oscillations in Metals* (Cambridge University Press, Cambridge, 1984).
- <sup>17</sup>A. G. Lebed, *Phys. Rev. Lett.* **74**, 4903 (1995).